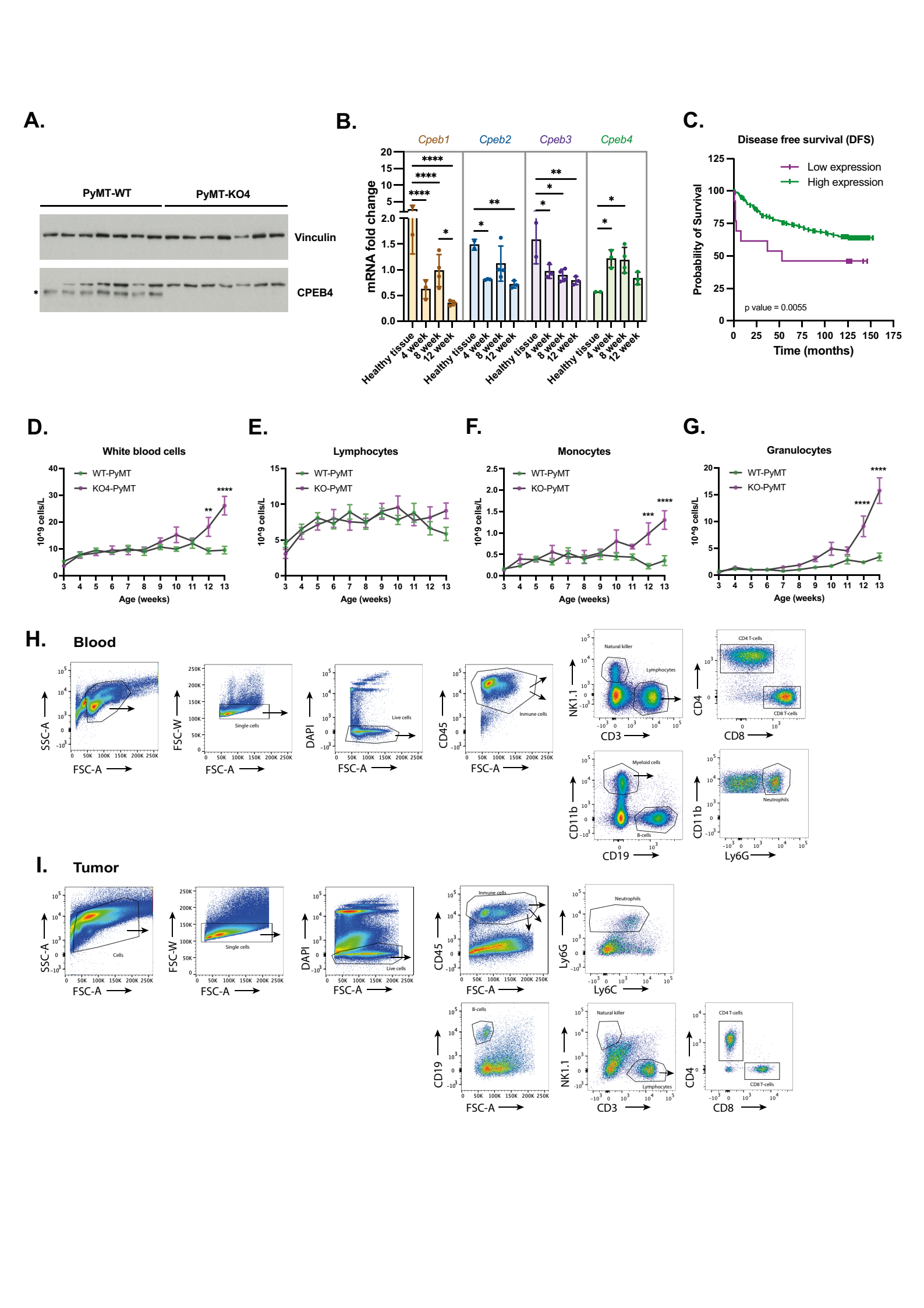
A.
PyMT-WT
PyMT-KO4
Vinculin
CPEB4
B.
Cpeb1
Cpeb2
Cpeb3
Cpeb4
mRNA fold change
Healthy tissue
4 week
8 week
12 week
C.
Disease free survival (DFS)
Low expression
High expression
Probability of Survival
p value = 0.0055
Time (months)
D.
White blood cells
E.
Lymphocytes
F.
Monocytes
G.
Granulocytes
WT-PyMT
KO4-PyMT
KO-PyMT
10^9 cells/L
Age (weeks)
H.
Blood
SSC-A
FSC-A
FSC-W
Single cells
DAPI
Live cells
CD45
Immune cells
NK1.1
CD3
Natural killer
Lymphocytes
CD4
CD8
CD4 T-cells
CD8 T-cells
CD11b
CD19
Myeloid cells
B-cells
Ly6G
Neutrophils
I.
Tumor
Cells
Ly6C

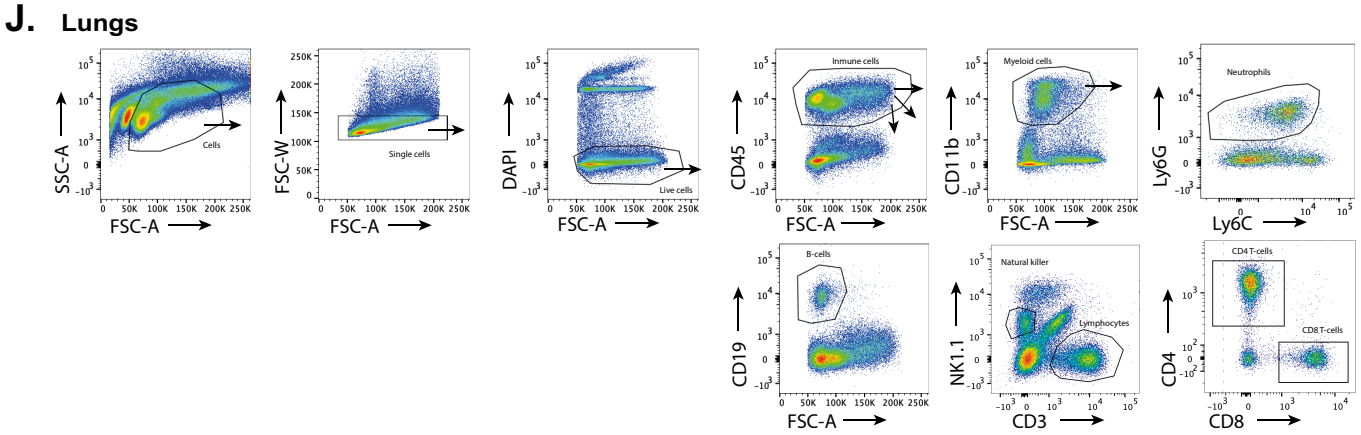
J. Lungs
SSC-A
FSC-A
Cells
FSC-W
Single cells
DAPI
Live cells
CD45
Inmune cells
CD11b
Myeloid cells
Ly6G
Ly6C
Neutrophils
CD19
B-cells
NK1.1
CD3
Natural killer
Lymphocytes
CD4
CD8
CD4 T-cells
CD8 T-cells

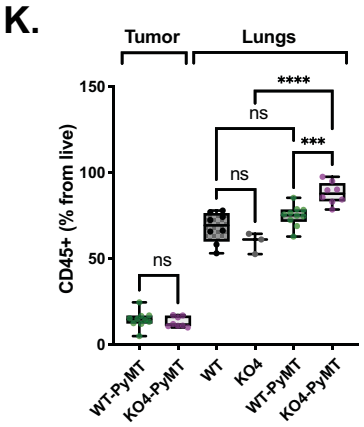
K.
Tumor
Lungs
CD45+ (% from live)
WT-PyMT
KO4-PyMT
WT
KO4

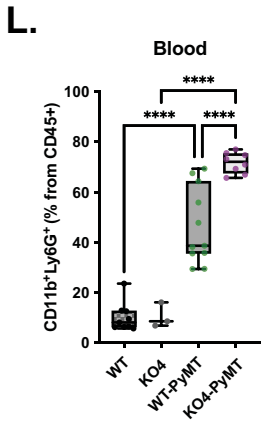
L.
Blood
CD11b+Ly6G+ (% from CD45+)
WT
KO4
WT-PyMT
KO4-PyMT

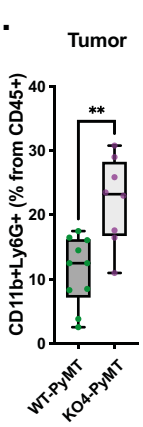
M.
Tumor
CD11b+Ly6G+ (% from CD45+)
WT-PyMT
KO4-PyMT

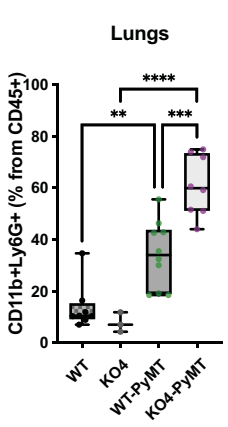
N.
Lungs
CD11b+Ly6G+ (% from CD45+)
WT
KO4
WT-PyMT
KO4-PyMT

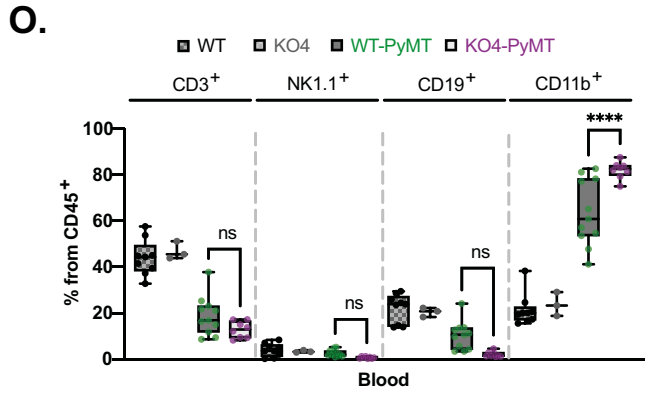
O.
WT
KO4
WT-PyMT
KO4-PyMT
CD3+
NK1.1+
CD19+
CD11b+
% from CD45+
Blood

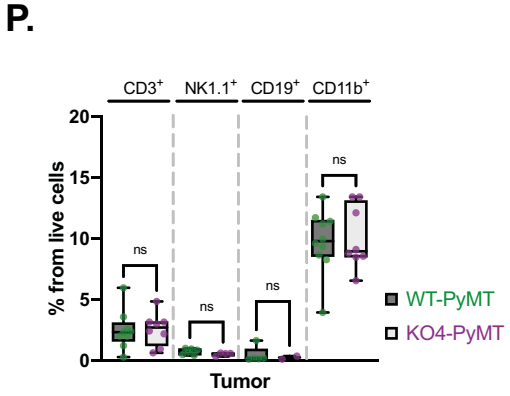
P.
CD3+
NK1.1+
CD19+
CD11b+
% from live cells
Tumor
WT-PyMT
KO4-PyMT

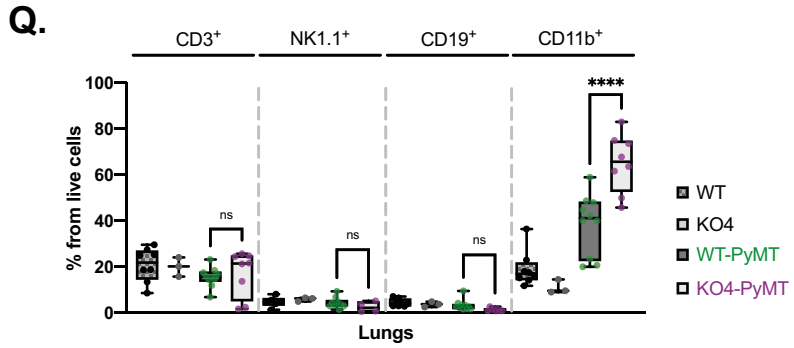
Q.
CD3+
NK1.1+
CD19+
CD11b+
% from live cells
Lungs
WT
KO4
WT-PyMT
KO4-PyMT

Extended Data Figure 1.

A. Western Blot of whole tumor lysates from WT-PyMT and KO4-PyMT breast tumors. CPEB4 protein levels are shown (*marks specific band). **B.** RT-qPCR showing *Cpeb1-4* mRNA levels in healthy tissue and in different stages of tumor progression (4, 8 and 12 week) in MMTV-PyMT mice model. **C**. Disease free survival (DSF) according to *Cpeb4* mRNA expression in the BCIP (Breast Cancer Integrative Platform) GSEA922_GPL97 dataset. **D, E, F, G**. Blood analysis of WT-PyMT and KO4-PyMT mice during tumor progression, from 3 to 13 weeks of age. White blood cells (B), lymphocytes (C), monocytes (D) and granulocytes (E) are shown. **H, I, J**. Gating strategy of flow cytometry analysis of immune cells present in blood (H), tumors (I) and lungs (J) from WT-PyMT and KO4-PyMT tumors. **K-Q**. Blood (L, O), tumors (K, M, P), and lungs (K, N, Q) of WT, KO4, WT-PyMT and KO4-PyMT mice analyzed by flow cytometry. (K) Immune cells infiltration in tumors and lungs is shown as % of $CD45^+$cells from total number of live cells in the tissue. (L, M, N) Neutrophil abundance is shown as % of $CD11b^+Ly6G^+$cells from total immune population ($CD45^+$). (O, P, Q) Relative abundance of lymphocytes ($CD3^+$), natural killer cells ($NK1.1^+$), B-cells ($CD19^+$) and myeloid cells ($CD11b^+$) shown as % of total immune cells ($CD45^+$) (O) or % of live cells (P, Q).

Data information: data are represented as mean ± s.d (B) or ± SEM (D-G). In (K-P) data are shown as a box (the median is middle band) with whiskers (min and max), where points represent individual mice. Statistical analysis was performed by two-way ANOVA (with Fisher's LSD test (B) or Šidák's correction (C-G)), one-way ANOVA (K, L, N-Q) or T-test (M). *P*-values *<0.05, **<0.01, ***<0.001, ****<0.0001 are indicated in the graphs; ns = not significant.

A.

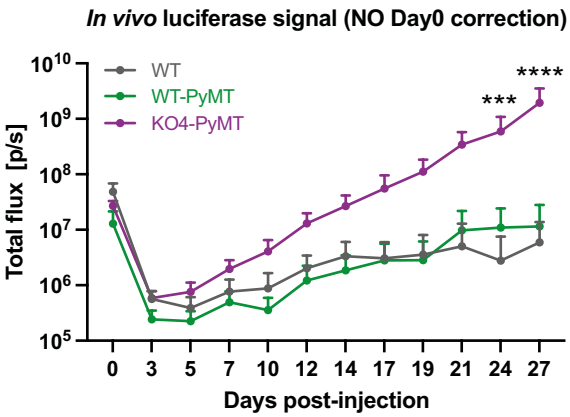
In vivo luciferase signal (NO Day0 correction)
WT
WT-PyMT
KO4-PyMT
****
***
Total flux [p/s]
10^{10}
10^{9}
10^{8}
10^{7}
10^{6}
10^{5}
0 3 5 7 10 12 14 17 19 21 24 27
Days post-injection

B.

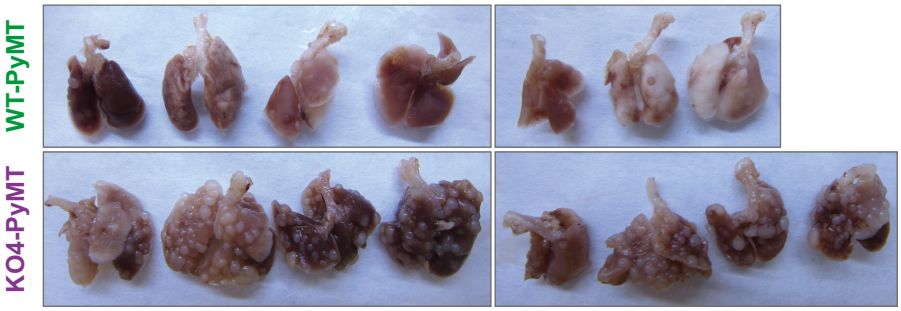
WT-PyMT
KO4-PyMT

C.

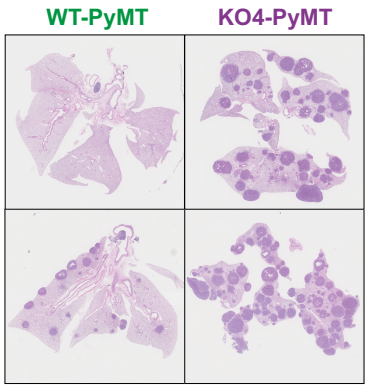
WT-PyMT
KO4-PyMT

Extended Data Figure 2.

A. *In vivo* quantification of bioluminescence signal (without day0 correction) of lung metastasis from WT, WT-PyMT and KO4-PyMT mice after tail-vein injection with peWT-PyMT-Luc cells. **B, C**. Images of lungs with macrometastasis (B) and representative H&E-stained lung sections from WT-PyMT and KO4-PyMT mice at day 27 post pePyMT-LUC cells injection.

Data information: data are represented as mean s.d. (A). Statistical analysis was performed by two-way ANOVA with Tukey correction (A). *P*-values ***<0.001, ****<0.0001 are indicated in the graphs.

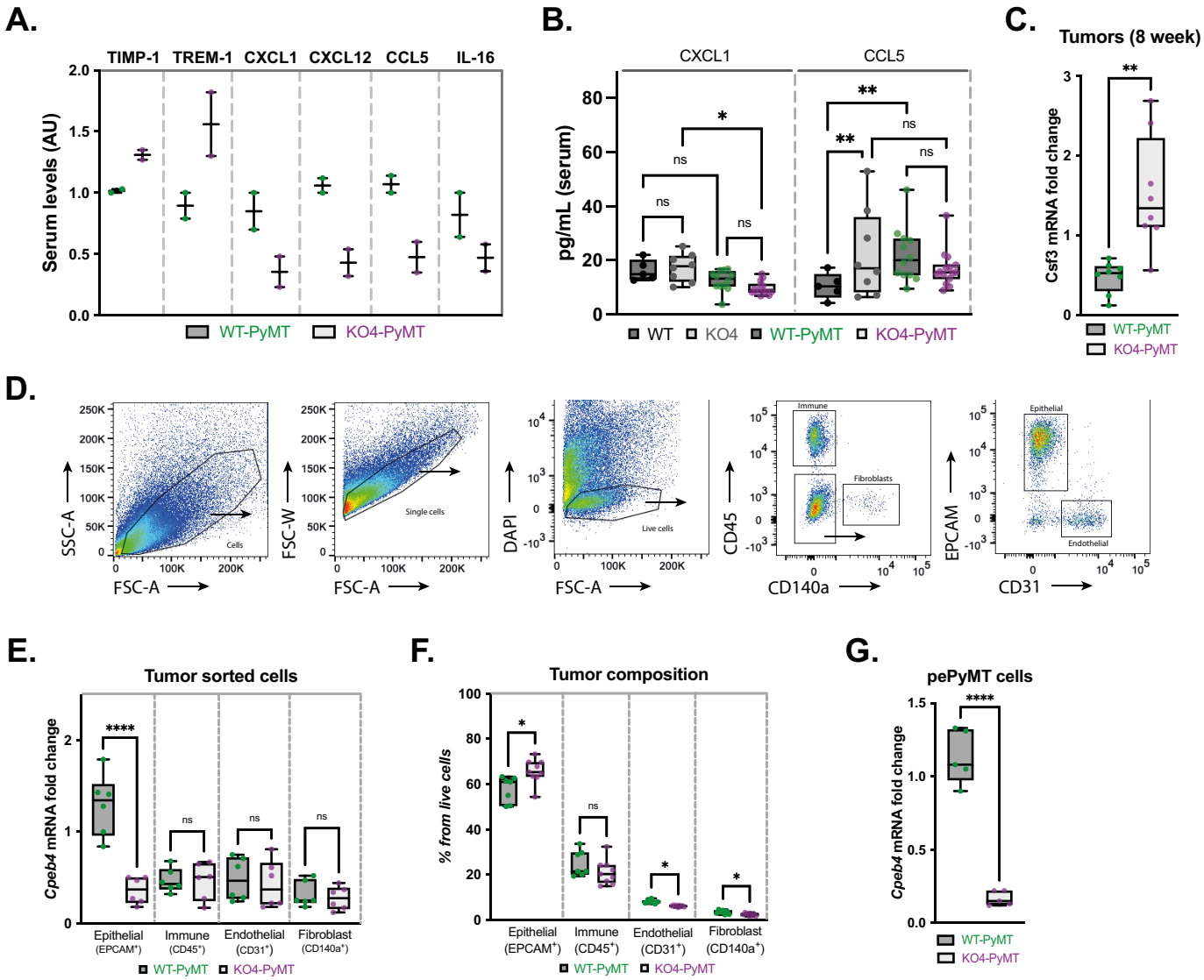
A.
TIMP-1
TREM-1
CXCL1
CXCL12
CCL5
IL-16
Serum levels (AU)
WT-PyMT
KO4-PyMT
B.
CXCL1
CCL5
pg/mL (serum)
ns
*
**
WT
KO4
WT-PyMT
KO4-PyMT
C.
Tumors (8 week)
Csf3 mRNA fold change
D.
SSC-A
FSC-A
Cells
FSC-W
Single cells
DAPI
Live cells
CD45
CD140a
Immune
Fibroblasts
EPCAM
CD31
Epithelial
Endothelial
E.
Tumor sorted cells
Cpeb4 mRNA fold change
****
Epithelial (EPCAM+)
Immune (CD45+)
Endothelial (CD31+)
Fibroblast (CD140a+)
F.
Tumor composition
% from live cells
G.
pePyMT cells

Extended Data Figure 3.

A. Quantification of cytokine arrays incubated with serum from WT-PyMT and KO4-PyMT mice (12 weeks). Differently expressed cytokines are shown. **B**. Quantification of CXCL1 and CCL5 levels in serum from WT, KO4, WT-PyMT and KO4-PyMT mice using Luminex MAGPIX system. **C**. RT-qPCR of whole tumor mRNA from WT-PyMT and KO4-PyMT mice at early stage of tumor progression (8 weeks). mRNA levels of *Csf3* are shown. **D**. Gating strategy of flow cytometry sorting of epithelial cells ($EPCAM^+$), immune cells ($CD45^+$), endothelial cells ($CD31^+$) and fibroblasts ($CD140a^+$) from WT-PyMT and KO4-PyMT tumors. **E**. RT-qPCR of *Cpeb4* mRNA levels in the different cell types present in the tumors (epithelial, immune, endothelial and fibroblasts), isolated by FACS-sorting after WT-PyMT and KO4-PyMT tumor disaggregation. **F**. Relative abundance of epithelial cells ($EPCAM^+$), immune cells ($CD45^+$), endothelial cells ($CD31^+$) and fibroblasts ($CD140a^+$) in WT-PyMT and KO4-PyMT tumors shown as % of total live cells. **G**. RT-qPCR showing *Cpeb4* mRNA levels in pePyMT from WT-PyMT and KO4-PyMT tumors after isolation and *ex vitro* culture.

Data information: data are shown as a box (the median is middle band) with whiskers (min and max), where points represent individual mice. Statistical analysis was performed by two-way ANOVA (B), T-test (C, G) ore one-way ANOVA (E, F). *P*-values *<0.05, **<0.01, ***<0.001, ****<0.0001 are indicated in the graphs; ns = not significant.

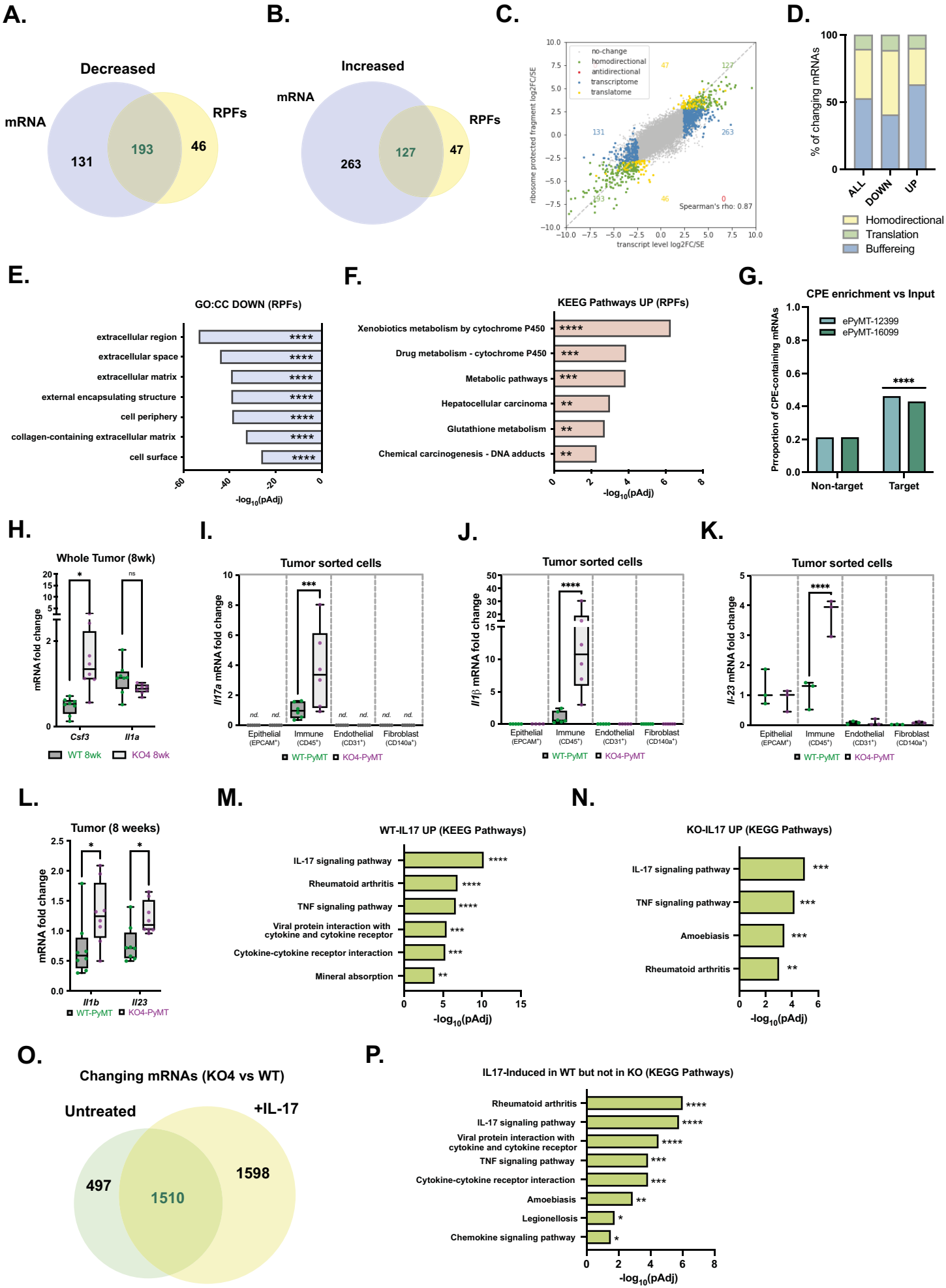
A.
Decreased
mRNA
RPFs
131
193
46
B.
Increased
mRNA
RPFs
263
127
47
C.
no-change
homodirectional
antidirectional
transcriptome
translatome
47
127
131
263
193
46
0
Spearman's rho: 0.87
ribosome protected fragment log2FC/SE
transcript level log2FC/SE
D.
% of changing mRNAs
ALL
DOWN
UP
Homodirectional
Translation
Buffereing
E.
GO:CC DOWN (RPFs)
extracellular region
extracellular space
extracellular matrix
external encapsulating structure
cell periphery
collagen-containing extracellular matrix
cell surface
-log10(pAdj)
F.
KEEG Pathways UP (RPFs)
Xenobiotics metabolism by cytochrome P450
Drug metabolism - cytochrome P450
Metabolic pathways
Hepatocellular carcinoma
Glutathione metabolism
Chemical carcinogenesis - DNA adducts
-log10(pAdj)
G.
CPE enrichment vs Input
Prroportion of CPE-containing mRNAs
ePyMT-12399
ePyMT-16099
Non-target
Target
H.
Whole Tumor (8wk)
mRNA fold change
Csf3
Il1a
WT 8wk
KO4 8wk
I.
Tumor sorted cells
Il17a mRNA fold change
Epithelial (EPCAM+)
Immune (CD45+)
Endothelial (CD31+)
Fibroblast (CD140a+)
WT-PyMT
KO4-PyMT
J.
Tumor sorted cells
Il1β mRNA fold change
K.
Tumor sorted cells
Il-23 mRNA fold change
L.
Tumor (8 weeks)
mRNA fold change
Il1b
Il23
M.
WT-IL17 UP (KEEG Pathways)
IL-17 signaling pathway
Rheumatoid arthritis
TNF signaling pathway
Viral protein interaction with cytokine and cytokine receptor
Cytokine-cytokine receptor interaction
Mineral absorption
N.
KO-IL17 UP (KEGG Pathways)
IL-17 signaling pathway
TNF signaling pathway
Amoebiasis
Rheumatoid arthritis
O.
Changing mRNAs (KO4 vs WT)
Untreated
+IL-17
497
1510
1598
P.
IL17-Induced in WT but not in KO (KEGG Pathways)
Rheumatoid arthritis
IL-17 signaling pathway
Viral protein interaction with cytokine and cytokine receptor
TNF signaling pathway
Cytokine-cytokine receptor interaction
Amoebiasis
Legionellosis
Chemokine signaling pathway

Extended Data Figure 4.

A, B. Venn diagram showing overlay of mRNAs decreased (A) or increased (B) at mRNA and ribosome protected fragment (RPF) level from a ribosome profiling analysis in WT-pePyMT and KO4-pePyMT cells. **C.** Scatter plot showing the classification of gene regulatory modes based on ribosome profiling data, as described in [50]. Genes are categorized into homodirectional regulation (green), where mRNA abundance and translation are coupled; translational buffering (blue), where changes in mRNA levels are offset by inverse changes in translation efficiency; and translational regulation (yellow), where mRNA levels remain unchanged, but translation efficiency is modulated. **D.** Bar plot showing the proportion of mRNAs regulated by each regulatoy mode specified in (C). **E, F**. Pathway enrichment analysis from genes with decreased (E) or increased (F) RPFs in KO4-PyMT vs WT-PyMT ePyMT cells in the Ribosome Profiling. Top pathways enriched from Gene Ontology:CC (location) (E) and KEGG pathway (F) collection database are shown. **G**. Comparison of percentage of genes containing CPE element in their 3′UTR in the whole mouse transcriptome versus RIP targets in 12399 and 16099 immortalized ePyMT cells. **H.** RT-qPCR of whole early stage (8 weeks) tumor samples. mRNA levels of *Csf3* and *Il1a* are shown. **I-K.** RT-qPCR of *Il17a* (I), *Il1β* (J) and *Il23* (K) mRNA levels in the different cell types present in the tumors (epithelial, immune, endothelial and fibroblasts). **L**. RT-qPCR of whole early stage (8 weeks) tumor samples. mRNA levels of *Il1b* and *Il23* are shown. **M, N**. RNA-seq pathway enrichment analysis from genes upregulated after IL-17A treatment in WT-pePyMT cells (M) and in KO4-pePyMT cells (N). Top pathways enriched from the KEGG pathway collection database are shown. **0**. Venn diagram showing RNA-seq overlay between significantly changing RNAs in KO4-pePyMT cells compared to WT-pePyMT in basal conditions and after IL-17A treatment. **P**. RNA-seq pathway enrichment analysis from genes significantly upregulated in WT but not in CPEB4 KO pePyMT cells upon IL-17A treatment. Top pathways enriched from the KEGG pathway collection database are shown.

Data information: data are shown as a box (the median is middle band) with whiskers (min and max), where points represent individual mice/sample (H-L). Statistical analysis was performed by multiple T-test (H, L) or one-way ANOVA (I-K). *P*-values/pAdj *<0.05, **<0.01, ***<0.001, ****<0.0001 are indicated in the graphs; ns = not significant.

A.

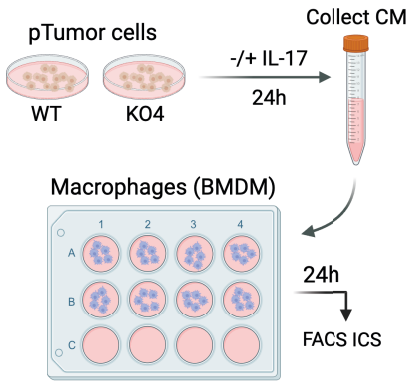
pTumor cells
Collect CM
-/+ IL-17
24h
WT
KO4
Macrophages (BMDM)
1
2
3
4
A
B
C
24h
FACS ICS

B.

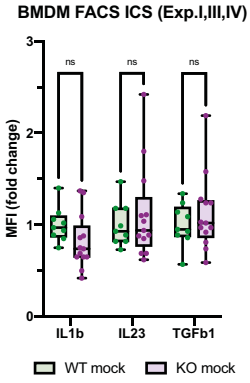
BMDM FACS ICS (Exp.I,III,IV)
MFI (fold change)
3
2
1
0
ns
ns
ns
IL1b
IL23
TGFb1
WT mock
KO mock

C.

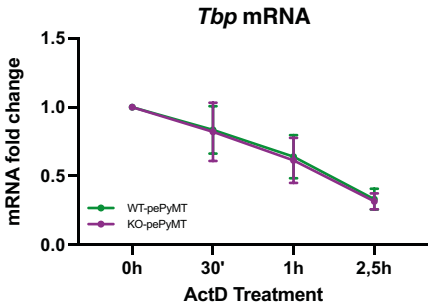
Tbp mRNA
mRNA fold change
1.5
1.0
0.5
0.0
WT-pePyMT
KO-pePyMT
0h
30'
1h
2,5h
ActD Treatment

Extended Data Figure 5.

A. Schematic representation of the experimental design for macrophage activation with tumor cell CM (created in BioRender. Mendez, R. (2025) https://BioRender.com/e53m553). **B.** FACS intracellular staining (ICS) of BMDM after activation with CM from WT and CPEB4 pePyMT cells**. C**. mRNA stability of *Tbp* mRNAs after actinomycin D (ActD) treatment in WT and Cpeb4 KO pePyMT cells. Gene expression analyzed by RT-qPCR and normalized to *Rplp0*.

Data information: data are shown as a box (the median is middle band) with whiskers (min and max) in (B) and as mean ±s.d in (C). Statistical analysis was performed by two-way ANOVA; ns = not significant.